

Original Article

Identification of miR-133a-3p-expression signature and probable mechanism in lung squamous cell carcinoma: Insights from integrated analysis

Lu Liang*, Yongyao Gu*, Yiwu Dang, Ping Li, Xiaoning Gan, Wenting Huang, Gang Chen, Dianzhong Luo

Department of Pathology, First Affiliated Hospital of Guangxi Medical University, Nanning, Guangxi, Zhuang Autonomous Region, China. *Equal contributors.

Received August 23, 2016; Accepted August 28, 2016; Epub October 1, 2016; Published October 15, 2016

Abstract: Lung squamous cell carcinoma (LUSC) is the second largest subtype of lung cancer and have been suggested decreased in cancers, but the mechanism is still elusive. The objective of this study was to investigate the role of miR-133a-3p in LUSC and reveal the potential mechanism related to miR-133a-3p. In Gene Expression Omnibus (GEO) database, miRNA microarrays involved in LUSC were collected to conduct a meta-analysis. The results were validated in clinical samples by qRT-PCR. The miRNA sequencing data in LUSC were collected from The Cancer Genome Atlas (TCGA), and the different expression of pri-miR-133a between LUSC and non-cancerous tissues were analyzed. In LUSC cell microarrays, deregulated genes associated with miR-133a-3p were collected, combined with the predicted target genes by online tools, we then searched for potential target genes of miR-133a-3p. The target genes were enriched by Gene Oncology (GO) and Kyoto Encyclopedia of Genes and Genomes (KEGG) pathway. Meta-analysis showed that miR-133a-3p was down-regulated in LUSC [SMD (95% CI)=-1.18 (-1.90, -0.45)]. TCGA data demonstrated that miR-133a-1 (P<0.001, the area under the ROC curve (AUC)=0.961) and miR-133a-2 (P<0.001, AUC=0.794) were down-regulated in LUSC. The results were consistent with clinical samples in house (P<0.001, AUC=0.801). Five-hundred-twenty genes were identified as potential target genes of miR-133a-3p. They were mainly enriched in GO terms referring to nucleotide regulation. Endocytosis was the most significantly enriched KEGG pathway. miR-133a-3p were downregulated in LUSC, act as a suppressive miRNA in LUSC. Nucleotide regulated and endocytosis may be the mechanisms by which miR-133a-3p acts on LUSC.

Keywords: Lung squamous cell carcinoma, miR-133a-3p, GEO, microarray, qRT-PCR

Introduction

Lung cancer has been the most frequent malignancy globally since the 1980s, accompanied by high mortality [1, 2]. Because lung cancer occurs silently and lacks an efficient diagnosis in the early stage, patients are always at an advanced stage when a definite diagnosis is made and have missed the opportunity to receive valuable treatments [3]. Compared with small cell lung cancer (SCLC), non-small cell lung cancer (NSCLC) forms the majority of lung cancers [4]. Adenocarcinoma (LUAD), lung squamous cell carcinoma (LUSC) and lung large cell cancer are subtypes of NSCLC. Until now, research on the molecular characteristics of LUSC has been less improved than that of lung LUAD. In LUAD, targeted agents, such

as EGFR, were discovered and applied in the clinic; however, in LUSC, no effective treatment has been found [5]. Thus, it is urgent to seek high-performance target genes in LUSC.

Aberrant molecular expression at the genome and transcriptome levels is a sign of cancer. microRNAs (miRNA, miR) are non-coding RNAs that are approximately 20 nucleotides in length [6]. They can bind to the 3'-untranslated region (3'-UTR) of corresponding messenger RNAs, regulate gene expression at the post-translational level [7], act as regulators in DNA expression [8], and sometimes interact with long non-coding RNAs [9]. Cumulative studies have reported that miRNAs are abnormally expressed in malignant tissues, blood or cells and act as suppressors or promoters in various cancers [10-12].

In humans, miR-133a-1 and miR-133a-2 are the precursors of miR-133a-3p and miR-133a-5p, which are transcribed from chromosomes 18q11.2 and 20q13.33, respectively. The accession number of miR-133a-3p is MIMAT00-00427. The common name “miR-133a” is miR-133a-3p [13]. Many studies have found that miR-133a is decreased in cancer tissues. Mirghasemi et al. [14] have found that miR-133a is down-expressed in osteosarcoma compared with adjacent normal bone tissues. The study of Zhang et al. [15] has suggested that miR-133a-3p presents at a lower level in hepatocellular carcinoma tissues than normal liver tissues. In a lung cancer study, Wang et al. [16] have revealed that miR-133a is down-regulated in NSCLC specimens, consistent with a recent study of our group [17]. However, few studies have focused on miR-133a expression in LUSC tissues, except for Mataki et al. [18]; however, the sample number in Mataki et al. [18] is too low to reveal the role of miR-133a-3p in LUSC. Thus far, the mechanism of miR-133a-3p in LUSC is unclear.

The aim of the present study was to investigate the role of miR-133a-3p in LUSC with a sizable dataset. To achieve this aim, we first collected suitable miRNA datasets from the Gene Expression Omnibus (GEO) database and conducted a meta-analysis. Profiles of miRNAs in LUSC were also obtained from The Cancer Genome Atlas (TCGA) and analyzed. Moreover, to validate the results, miR-133a-3p in LUSC specimens was detected by qRT-PCR. Finally, potential target genes of miR-133a-3p were searched for in the GEO datasets and online predicted tools. Functional annotation of the target genes was performed by Gene Ontology (GO) and Kyoto Encyclopedia of Genes and Genomes (KEGG) pathway analyses.

Methods and materials

Meta-analysis procedure

miRNA microarray datasets were downloaded from the Gene Expression Omnibus (GEO) DataSets (<http://www.ncbi.nlm.nih.gov/gds>). The searched terms were directed at lung cancer and organisms were limited to Homo sapiens. The titles and abstracts of the searched datasets were reviewed by two researchers independently. The studies referring to miRNA detection were picked for further assessment. The included criteria were as follows: 1. LUSC subtypes; indistinct subtypes

were excluded. 2. Microarray samples were from LUSC tissue; blood and cell line studies were excluded. 3. The expressed intensity of miR-133a-3p was provided. 4. Normal controls were designed in the study. The data files of the included studies were downloaded, and the processed data were used to pool the effect sizes. Additionally, raw data were downloaded, and background correction and normalization between the arrays were processed by the ExiMiR (spike-in array) [19] or limma [20] package of R software. The basic information of the included studies was extracted by two investigators independently. Contradictions were resolved by discussions with other researchers. The standard mean difference (SMD) and corresponding 95 percent confidence intervals (95% CI) were estimated and pooled by Stata 12.0. Heterogeneity between studies was assessed by inconsistency squared (I^2) and chi-squared tests. An I^2 value less than 50% and a p value more than 0.05 were considered to be inconspicuous heterogeneity, and then, the fixed effect model was applied to pool the effect size. Subgroup analysis and sensitivity analysis were performed to research the source of heterogeneity.

Analysis of the pri-miR-133a status in LUSC from TCGA

The profiles of pri-miRNAs, including miR-133a-1 and miR-133a-2 in LUSC, were available from the miRNA-seq database of The Cancer Genome Atlas (TCGA). The level 3 data were downloaded from the TCGA data portal on August 2016. The data of the reads per million miRNAs mapped were used to analyze the discrepancy of the pri-miRNA level between LUSC and normal lung tissues.

The different pri-miR-133a expression levels between the LUSC and normal groups were analyzed by Student's t test and $P < 0.05$ indicated a statistically significant difference. The data were calculated by SPSS 20.0, and the figures were constructed using Graphpad prism 5.0.

The source of tissue samples

LUSC tissues were collected from 23 patients who had undergone operation at the First Affiliated Hospital of Guangxi Medical University between January 2012 and February 2014. Corresponding adjacent non-cancerous lung tissues were collected as well. All of the tissue

miR-133a-3p in lung squamous cell carcinoma

Table 1. Information of included studies in meta-analysis

ID	Platform ID	Country	Update year	Sample source	Sample size	
					Tumor	Control
GSE16025	GPL5106	USA	2012	Tissues	60	10
GSE18696	GPL4717 GPL4718	France	2015	Tissues	6	6
GSE25508	GPL7731	Finland	2016	Tissues	8	8
GSE29248	GPL8179	China	2014	Tissues	3	3
GSE47525	GPL17222	Netherlands	2015	Tissues	4	8
GSE51853	GPL7341	Japan	2016	Tissues	29	5
GSE56036	GPL15446	Japan	2015	Tissues	6	6
GSE74190	GPL19622	China	2015	Tissues	30	11

Screening the target genes of miR-133a-3p

In the GEO DataSets, two studies (GSE26032, GSE56243) were found to explore differentially expressed genes (DEGs) in LUSC cell lines with transfected miR-133a-3p. The cell lines in GSE26032 were H157 and P10, and EBC-1 and SK-MES-1 were included in

samples were conserved by formalin-fixed, paraffin-embedded (FFPE). Two pathologists reviewed each sample and confirmed the diagnosis. Discrepancies were solved by another pathologist or by conference. The age range of the patients was from 23 to 82 years and included 18 male and 5 female patients. Written informed consent was received from all of the patients.

Quantitative RT-PCR array for miR-133a-3p expression

After the FFPE sections were dewaxed and incubated, total RNA was extracted with the miRNeasy FFPE Kit (QIAGEN, KJVenlo, the Netherlands) as described previously [21]. The RNA concentration was detected using a Nanodrop 2000 (Wilmington, DE, USA). miR-191 (Forward: 5'-CAACGGAAUCCCAAAGCAGCU) and miR-103 (Forward: 5'-AGCAGCAUUGUACAGGGCUAUGA) were used as control miRNAs for stable expression according to Norm-Finder and geNorm. In TaqMan microRNA assays, primers for miR-133a (Forward: 5'-UUGGUCCCUUCAACCAGCUGU), control miRNAs and reverse primers were included. The TaqMan MicroRNA Reverse Transcription kit was used for reverse transcription, and an Applied Biosystems PCR7900 (miR-133a: Cat. No. 44-27975-000458, miR-191: Cat. No. 4427975-000490, miR-103: Cat. No. 4427975-000439) was used to perform real-time quantitative PCR according to the manufacturer's instructions. The relative expression of miR-133a was calculated by the formula $2^{-\Delta Cq}$ [22].

The different expression levels of miR-133a-3p between LUSC and normal groups were tested by Student's t test and $P < 0.05$ was considered to be statistically significant. The data were calculated by SPSS 20.0, and figures were constructed using Graphpad prism 5.0.

GSE56243. The four cell lines were explored in two-color microarrays with negative controls. To screen the DEGs, the processed data (log₁₀ ratio normalized) were transformed to the fold change. Genes with more than 1.45-fold up- or down-expressed changes ($P < 0.01$) were collected from each of the four datasets. To reduce the gene heterogeneity from the different cell lines, DEGs overlapping in at least $\frac{3}{4}$ of the sets were collected. Meanwhile, 13 web servers (miRWalk, MicroT4, miRanda, mirbridge, miRDB, miRMap, miRNAMap, Pictar2, PITA, RNA22, RNAhybrid, Targetscan and mirTarbase) were used to predict the target genes of miR-133a-3p. Genes co-predicted on at least five web servers were collected. Genes included in the DEGs acquired from microarrays were also contained in target genes predicted by web servers and were considered to be the target genes of miR-133a-3p.

Functional annotation of genes targeted by miR-133a-3p

To explore the potential function of miR-133a-3p in LUSC, the target genes were analyzed by Gene Ontology (GO) analysis and the Kyoto Encyclopedia of Genes and Genomes (KEGG) pathway in DAVID (<https://david.ncifcrf.gov/>). The BINGO plug-in of Cytoscape was used in GO analysis as well.

Results

Meta-analysis of miR-133a-3p expressed in LUSC

According to the search strategy and included criteria mentioned above, eight datasets from the GEO Database were enrolled in the meta-analysis, comprising 146 LUSC and 57 normal lung tissue samples. The basic information of the enrolled studies is shown in **Table 1**. By region, four studies (GSE29248,

miR-133a-3p in lung squamous cell carcinoma

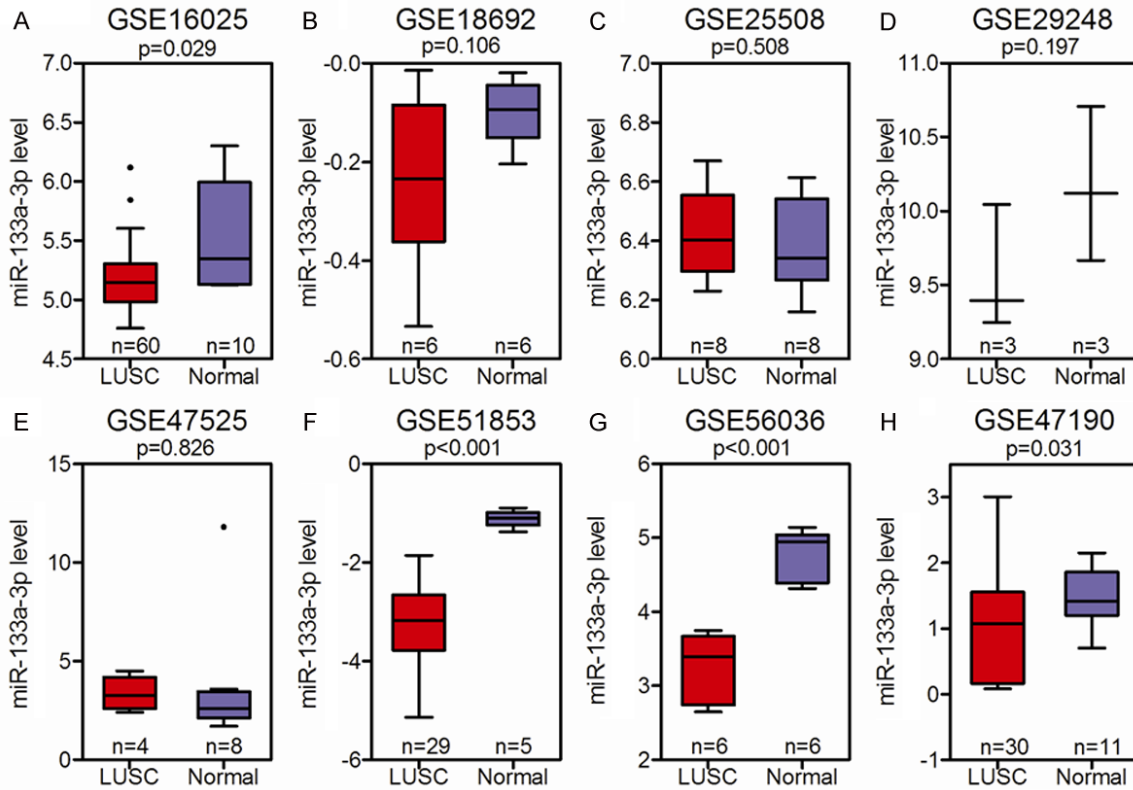


Figure 1. Different expression levels of miR-133a-3p between lung squamous cell carcinoma tissues and normal lung tissues in the included datasets of the meta-analysis. The center line in the box represents the mean value of miR-133a-3p expression. The two ends of the box represent the upper (25%) quartile and lower (75%) quartile. The two lines outside the box represent the 95% confident intervals (CIs). Dots outside the box represent outliers. LUSC: lung squamous cell carcinoma.

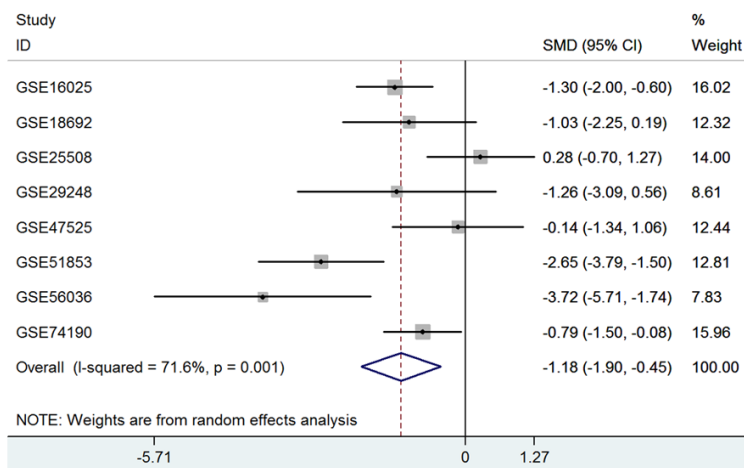


Figure 2. Forest plot assessing the miR-133a-3p level in lung squamous cell carcinoma tissues by the random-effects model. The pooled standard mean difference was -0.18, and the 95% confident interval (-1.90, -0.45) suggested that miR-133a-3p was deregulated in lung squamous cell carcinoma tissues.

one (GSE16025) was from America. The different expression levels of miR-133a-3p between LUSC and normal controls in each dataset are displayed in **Figure 1**. To validate the result of decreased miR-133a-3p in LUSC, we pooled SMD and 95% CIs with the extracted data of all of the enrolled studies. If significant heterogeneity ($I^2=71.6\%$, $P=0.001$) was detected, SMD was calculated by the random effect model. The pooled SMD (-1.18) and 95% CI (-1.90, -0.45) showed that low miR-133a-3p expression was correlated with LUSC (**Figure 2; Table 2**).

GSE51853, GSE56036 and GSE74190) were from Asia, three studies (GSE18696, GSE-25508 and GSE47525) were from Europe, and

To investigate whether there were different results in different regions, subgroup analysis based on region was performed. In three

miR-133a-3p in lung squamous cell carcinoma

Table 2. Meta-analysis of miR-133a-3p in lung squamous cell carcinoma by random effect model

ID	Cancer group			Control group			Weight (%)	SMD (95% CI)
	N	Mean	SD	N	Mean	SD		
GSE16025	60	5.16529	0.249596	10	5.533700	0.445945	16.02	-1.30 (-2.00, -0.60)
GSE18696	6	-0.23851	0.178682	6	-0.09976	0.067497	12.32	-1.03 (-2.25, 0.19)
GSE25508	8	6.424836	0.155679	8	6.380495	0.160236	14.00	0.28 (-0.70, 1.27)
GSE29248	3	9.564713	0.425075	3	10.16542	0.521892	8.61	-1.26 (-3.09, 0.56)
GSE47525	4	3.35000	0.866025	8	3.7375	3.310562	12.44	-0.14 (-1.34, 1.06)
GSE51853	29	-3.28627	0.874981	5	-1.11513	0.172442	12.81	-2.65 (-3.79, -1.50)
GSE56036	6	3.267231	0.469411	6	4.794464	0.341339	7.83	-3.72 (-5.71, -1.74)
GSE74190	30	0.960483	0.737446	11	1.493247	0.453641	15.96	-0.79 (-1.50, -0.08)
Total	146			57			100	-1.18 (-1.90, -0.45)

N: Sample size; SD: Standard Deviation; SMD: Standard Mean Difference; CI: Confidence Interval.

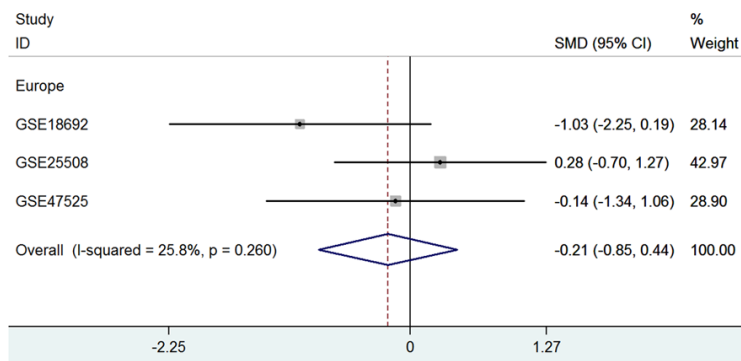


Figure 3. Forest plot assessed the miR-133a-3p expression level in lung squamous cell carcinoma tissues from Europe. The standard mean difference (-0.21) and 95% confident interval (-0.85, 0.44) suggested that the expression of miR-133a-3p showed no significant change in lung squamous cell carcinoma.

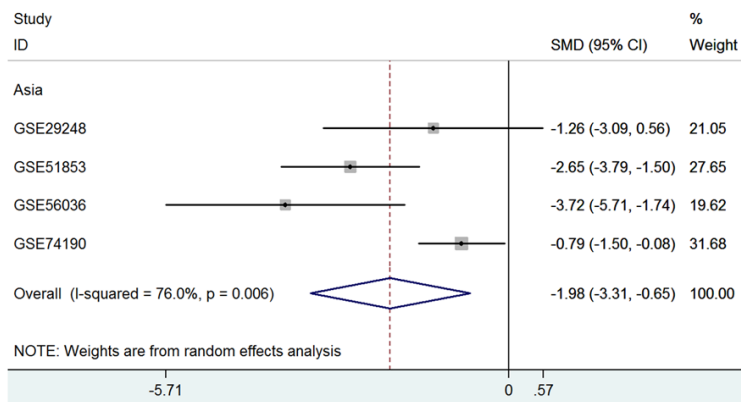


Figure 4. Forest plot assessed miR-133a-3p expression in lung squamous cell carcinoma tissues from Asia. The Pooled Standard Mean Difference (-1.37) and 95% confident interval (-2.28, -0.46) suggested that miR-133a-3p was deregulated in lung squamous cell carcinoma tissues.

studies from Europe, the heterogeneity was insignificant ($I^2=25.8\%$, $P=0.260$); thus, the SMD was pooled by the fixed-effects model. As

shown in **Figure 3**, in European patients, no different miR-133a-3p expression was found between LUSC tissues and normal control samples (SMD: -0.21, 95% CI: -0.85~0.44). In microarrays from Asia, the heterogeneity was still significant ($I^2=76.0\%$, $P=0.006$). The pooled SMD (-1.98) and 95% CI (-3.31~-0.65) suggested that miR-133a-3p was down-regulated in LUSC tissues compared with that in normal lung tissues (**Figure 4**).

Sensitivity analysis showed that no study led to heterogeneity dominantly (**Figure 5**). Begg's funnel plot (**Figure 6**, $P=0.536$) and Egger's test ($P=0.416$) suggested that no publication bias existed in this meta-analysis.

Expression of pri-miR-133a in LUSC

Meanwhile, the expression of miR-133a-1 and miR-133a-2 in LUSC tissues was explored. Data were obtained from TCGA. miR-133a-1 was detected in a cohort including 336 LUSC and 44 normal lung tissues. miR-133a-2 was detected in another cohort

including 131 LUSC and 44 normal lung tissues. Compared with normal lung tissues, the miR-133a-1 and miR-133a-2 levels in LUSC

miR-133a-3p in lung squamous cell carcinoma

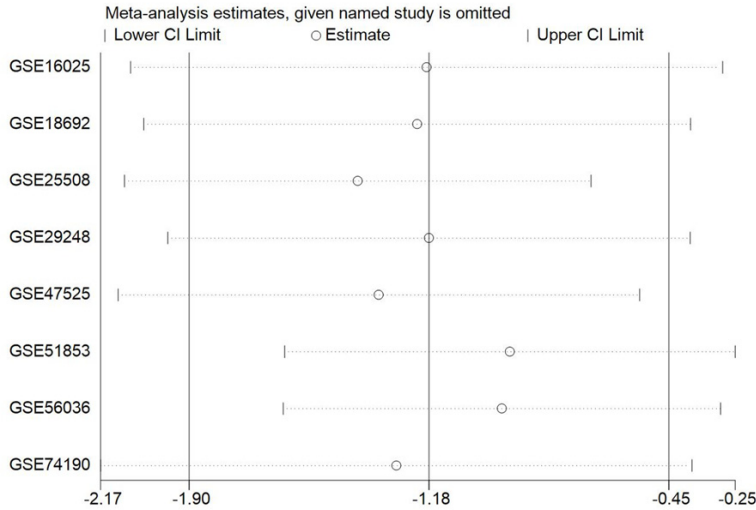


Figure 5. Sensitivity analysis of the miR-133a-3p expressed intensity in LUSC tissues. No study was found to obviously contribute to the heterogeneity.

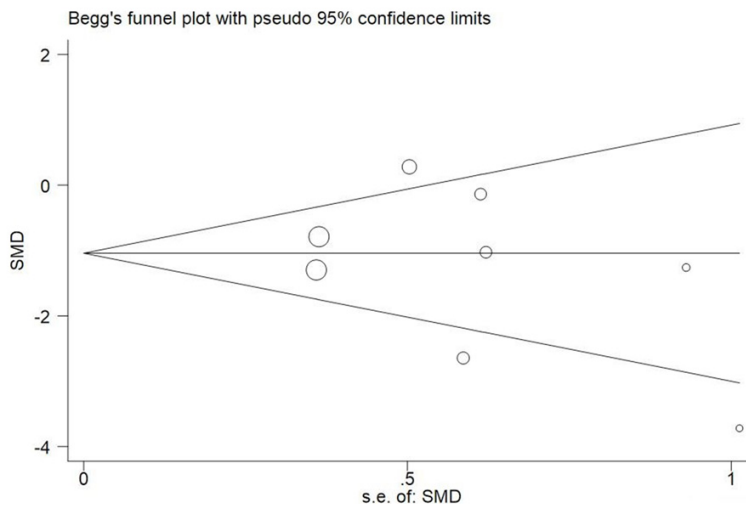


Figure 6. Begg's funnel plot show the publication bias of the included studies in meta-analysis. The dots were distributed symmetrically in the plot, indicating that the publication bias was insignificant.

were reduced 5.28-fold ($P < 0.001$) and 2.44-fold ($P < 0.001$), respectively. Receiver operating characteristic (ROC) curve analyses were also performed to evaluate the diagnostic value of miR-133a-1 and miR-133a-2 in LUSC, and the area under the curve (AUC) of the ROC curves for miR-133a-1 and miR-133a-2 in LUSC were 0.961 and 0.794, respectively (**Figure 7**).

Validation of the expression of miR-133a-3p in LUSC tissues

To validate the results of the meta-analysis, we detected the expression mature miR-133a-3p

by qRT-PCR in 23 LUSC tissues and paired adjacent lung tissues. The results showed decreasing miR-133a-3p expression in LUSC tissues (1.95-fold, $P < 0.001$) compared with that in adjacent lung tissues. The AUC of the corresponding ROC curve was 0.801 (**Figure 8**).

Target genes of miR-133a-3p

To further investigate the role of miR-133a-3p in LUSC, genes correlated with miR-133a-3p were sought synthetically. After two datasets (GSE26032, GSE56243) were processed as described in the Methods section, we obtained 1,842 DEGs. In total, 3995 predicted genes were acquired from 13 web servers. Finally, the DEGs achieved in the microarrays and genes predicted by the web servers were combined to run in the intersection. Finally, 520 potential target genes of miR-133a-3p were obtained.

Functional annotation of genes potentially targeted by miR-133a-3p

To classify the 520 potential target genes of miR-133a-3p by function, GO analysis was performed using the BINGO plug-in of Cytoscape and DAVID. Regarding the cellular components, the genes were enriched in intracellular parts, such as organelles; cell parts, such as the cytoskeleton; as well as the anchoring junction (**Figure 9**). For biological processes, significantly enriched terms were related to cellular processes, gene metabolism and organization (**Figure 10**). Regarding molecular function as described in **Figure 11**, most of the genes were assigned to binding, including nucleotide binding, cytoskeletal protein binding, and actin binding. GO-enriched terms were shown in networks constructed by BINGO (**Figure**

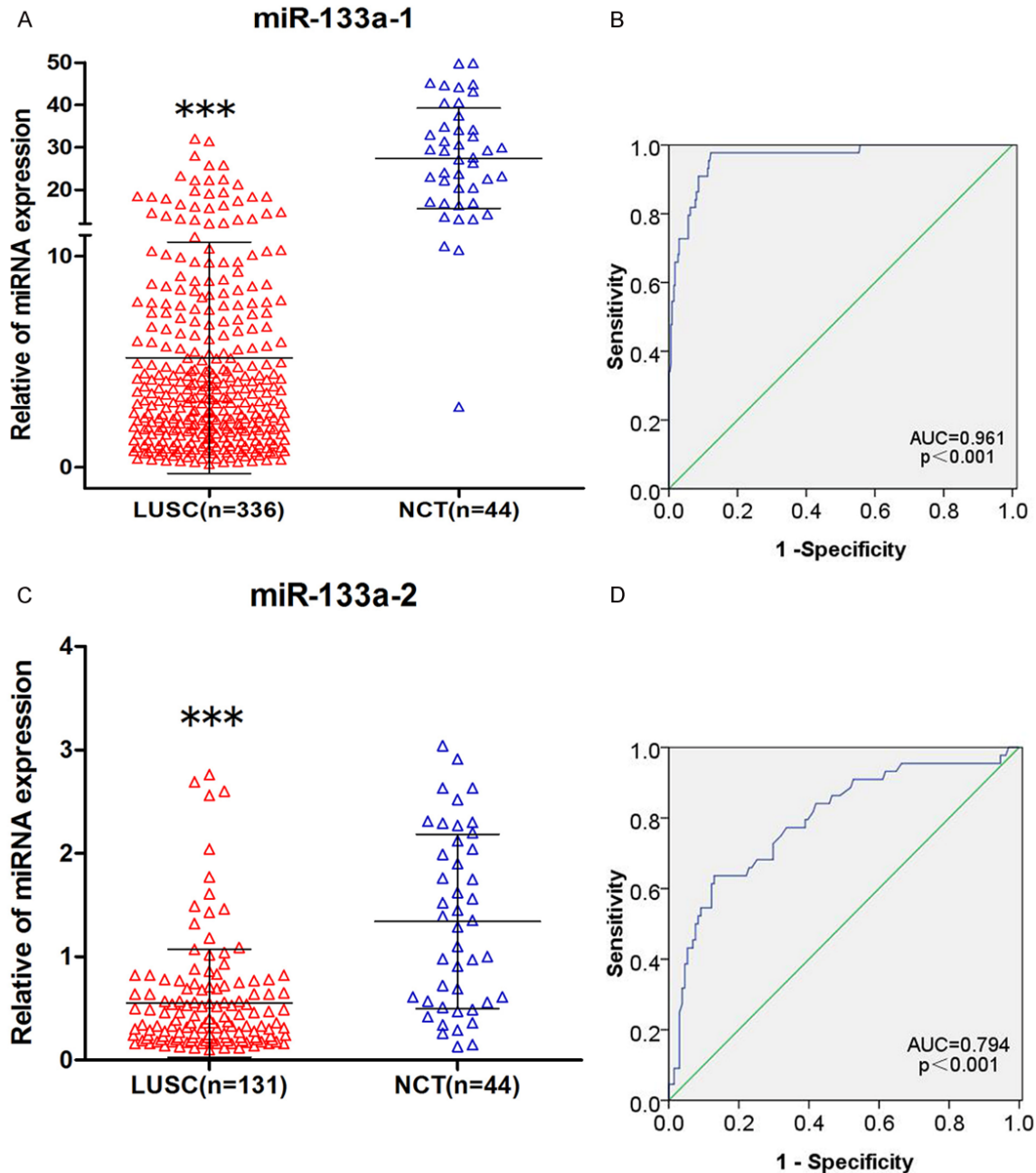


Figure 7. Precursors of the miR-133a-3p expressed signature in lung squamous cell carcinoma tissues (data from TCGA) and corresponding receiver operating characteristic curves. A. Different expression levels of miR-133a-1 in LUSC and non-cancerous lung tissues ($P < 0.001$). B. Diagnostic value of miR-133a-1 in lung squamous cell carcinoma (AUC=0.961, $P < 0.001$); C. Different expression levels of miR-133a-2 in LUSC and non-cancerous lung tissues ($P < 0.001$). D. Diagnostic value of miR-133a-2 in lung squamous cell carcinoma (AUC=0.794, $P < 0.001$). LUSC: lung squamous cell carcinoma; NCT: non-cancerous lung tissues; n: sample size; AUC: area under the curve. *** $P < 0.001$.

12). KEGG pathway enrichment analysis was performed by DAVID. The most significantly enriched pathway was endocytosis ($P = 0.0048$), which was enriched with 15 genes. The other significant enriched pathways are showed in Table 3.

Discussion

LUSC is one of the subtypes of NSCLC, accounting for 30% of NSCLC cases and resulting in approximately 400,000 deaths every year [23]. Much work has been conducted regarding the

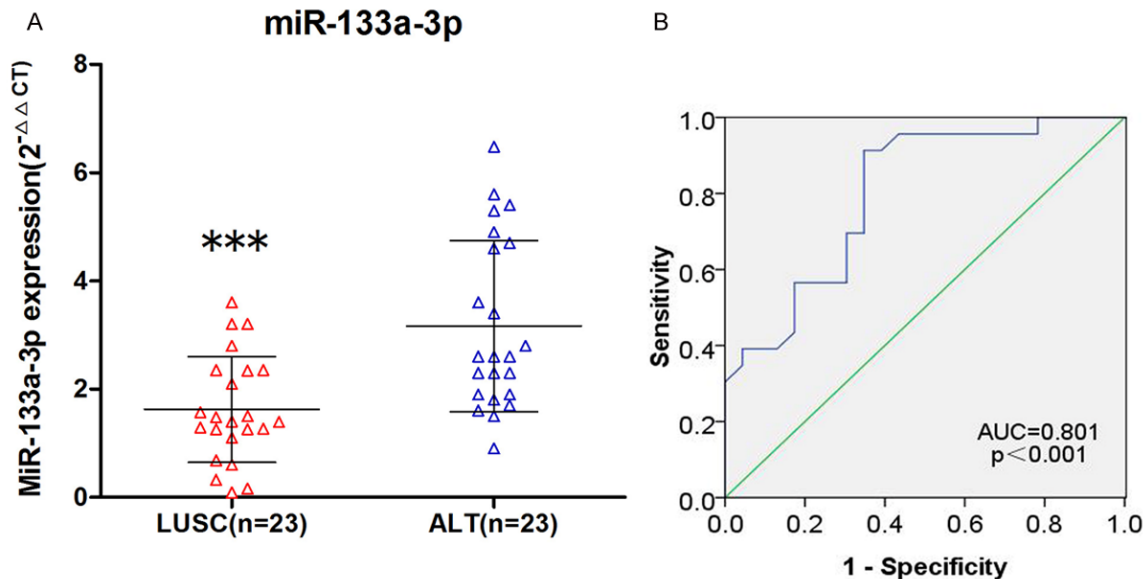


Figure 8. The miR-133a-3p expressed signature in lung squamous cell carcinoma tissues and corresponding receiver operating characteristic curve. A. Different expression levels of miR-133a-3p in LUSC and non-cancerous lung tissues ($P<0.001$). B. Diagnostic value of miR-133a-3p in lung squamous cell carcinoma (AUC=0.801, $P<0.001$). *LUSC: lung squamous cell carcinoma; NCT: non-cancerous lung tissues; n: sample size; AUC: area under the curve. *** $P<0.001$.

molecular mechanism of LUSC for several decades; however, the 5-year survival rate of LUSC patients remains low. More recently, many published studies have focused on non-coding RNAs in LUSC [24-26]. As a type of non-coding RNA, miRNAs have become a hotspot in LUSC research. Microarrays and qRT-PCR are currently the main methods to detect miRNAs [27, 28], and screening differently expressed miRNAs is a common process in these studies. Although many differently expressed miRNAs are screened, the corresponding mechanism remains unclear. To discover effective biomarkers to diagnose and treat LUSC, more studies are needed to elucidate the mechanism related to miRNAs in LUSC.

A recent report by our group found that miR-133a-3p is significantly decreased in NSCLC tissues compared with that in normal lung tissues [17]. A uniform trend is also found in the serum samples of NSCLC patients [29, 30]. In functional research for NSCLC, Wang et al. [31] demonstrated that miR-133a targets multiple oncogenic receptors in the membrane, such as EGFR, TGFBR1 and IGF-1R, and restricts the biological activity of cancer cells through corresponding pathways.

In this study, consistent results were obtained using different methods. First, a meta-analysis concerning miR-133a-3p expression in LUSC was performed using the GEO datasets. Despite different datasets with different results, we determined that miR-133a-3p is decreased in LUSC tissues after the data were pooled. Furthermore, data from TCGA suggested that miR-133a-1 and miR-133a-2 are both deregulated in LUSC tissues. As precursors of mature miR-133a-3p, this result is consistent with that of the meta-analysis. The results of the meta-analysis were validated in LUSC samples by qRT-PCR and were also supported by the study of Moriya et al. [13]. They tested miR-133a-3p in 25 pairs of LUSC and non-cancerous lung tissues, validating the tumor suppressor role of miR-133a-3p in LUSC cells. In gene expression analysis by microarrays (GSE26032), Moriya et al. [13] analyzed gene expression in LUSC cells transfected with miR-133a-3p and compared it with negative transfection cells. They finally suggested that ARPC5 and GSTP1 are notably regulated by miR-133a. It is worth noting that the dataset GSE26032 is one of the included datasets used to search for target genes of miR-133a-3p in the current study. Compared with Moriya et al. [13], synthetically analyzing the data from the public databases

miR-133a-3p in lung squamous cell carcinoma

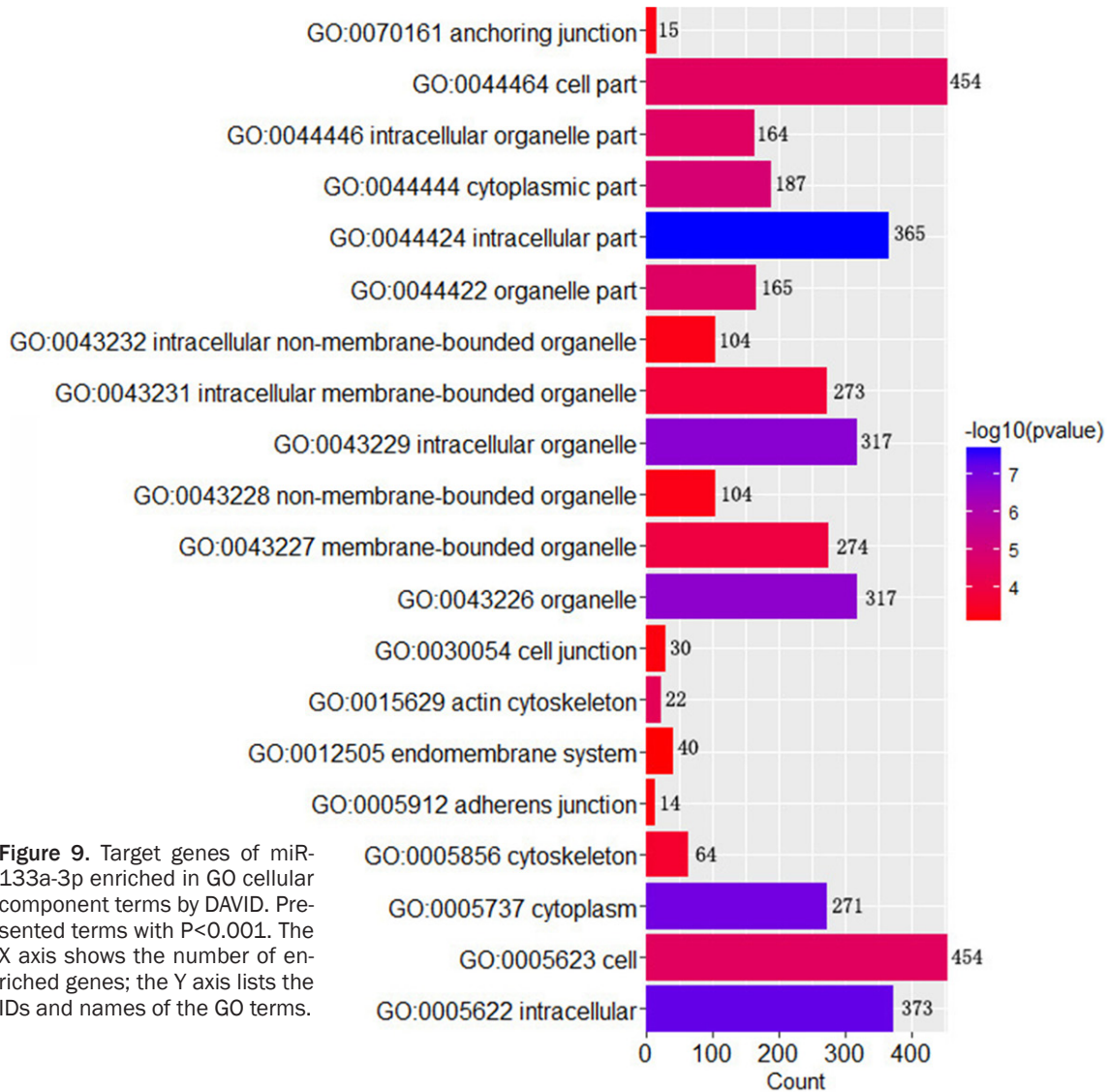


Figure 9. Target genes of miR-133a-3p enriched in GO cellular component terms by DAVID. Presented terms with $P < 0.001$. The X axis shows the number of enriched genes; the Y axis lists the IDs and names of the GO terms.

made the result more credible in our study. In another reported study, the miR-1/133a cluster was found to restrict migration and invasion, as well as the proliferation of LUSC cell lines [18].

It is known that miR-133a is decreased in several cancers and plays a role as a tumor suppressor, including in hepatocellular carcinoma (HCC) [15], breast cancer [32] and bladder cancer [33]. However, there are different mechanisms to contribute to cancers. For example, miR-133a can target Uncoupling Protein 2 (UCP-2) and down-regulate UCP-2 expression, leading to doxorubicin-sensitive breast cancer cells [32]. In hepatocellular carcinoma, miR-133a targets IGF-1R and suppresses the growth of HCC cells [15].

To further investigate the role of miR-133a-3p in LUSC, 520 potential target genes of miR-133a-3p were sought synthetically based on DEG analytic microarrays and sequence-based predicted tools. To research the mechanism of miR-133a-3p, the 520 potential target genes of miR-133a-3p were enriched by GO and KEGG pathway analyses in this study. Most of the enriched GO terms referred to nucleotide regulation. Aberrant nucleotide synthesis or deletion may lead to the deregulation of cell growth, which is very important in gene repair and tumorigenesis. For example, single-nucleotide polymorphisms (SNPs) in genes are related to the outcome of cancer patients. In advanced NSCLC patients, SNPs in the miRNA binding site of the MDM4 gene have a prognostic pre-

miR-133a-3p in lung squamous cell carcinoma

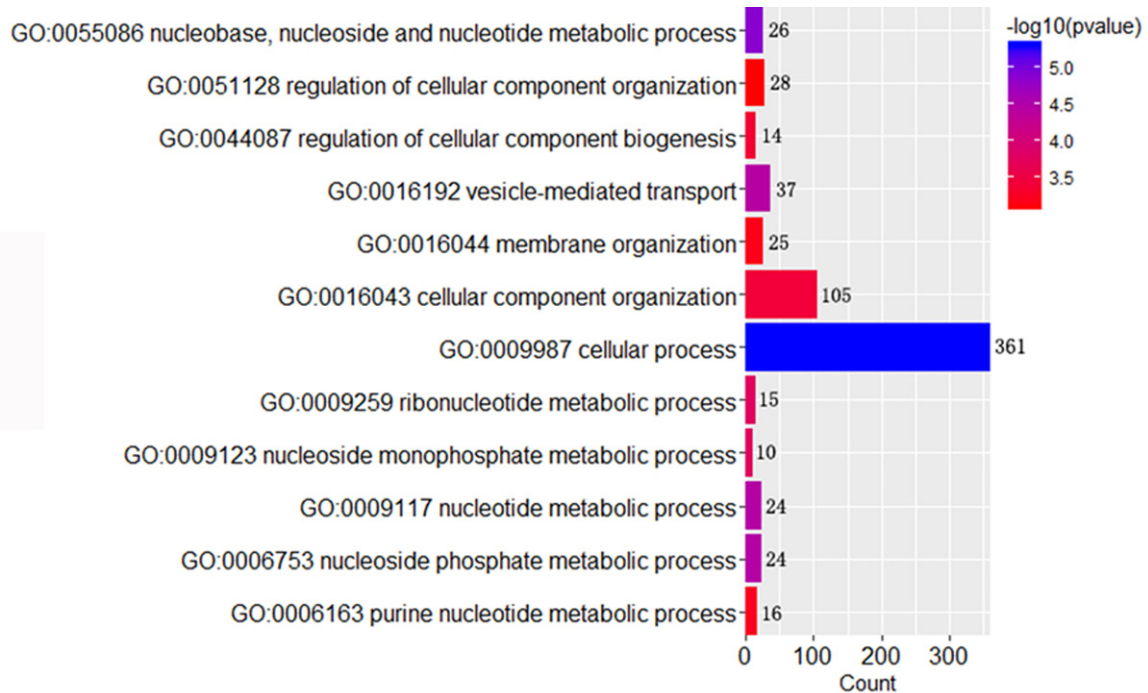


Figure 10. Target genes of miR-133a-3p enriched in the GO biological process terms by DAVID. Presented terms with $P < 0.001$. The X axis shows the number of enriched genes; the Y axis lists the IDs and names of the GO terms.

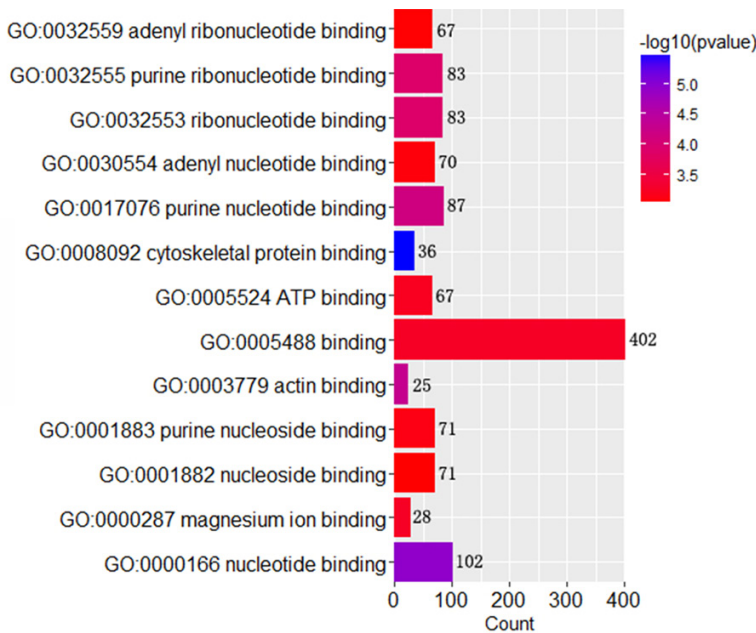


Figure 11. Target genes of miR-133a-3p enriched in the GO molecular function terms by DAVID. Presented terms with $P < 0.001$. The X axis shows the number of enriched genes; the Y axis lists the IDs and names of the GO terms.

KEGG pathway enrichment, target genes were enriched in seven significant pathways. Known pathways related to cancer, such as the p53 and mTOR signaling pathways, were included in significantly enriched pathways. The most significantly enriched term is endocytosis, which is a common transport mode in eukaryotic cells. Studies have found that endocytosis also participates in tumorigenesis through the resurrection of apoptotic cancer stem cells [35]. It was demonstrated that the endocytosis of oligonucleotides can be promoted by hydrogen peroxide, followed by the restraint of migration and invasion of cancer cells through calcium release [36]. The miR-199 family is reported to regulate

dicted value [34]. Interestingly, as members of the same family, MDM2 is a potential target gene of miR-133a-3p in the current study. In

endocytosis by controlling CLCT, Rab5A, LDLR and Cav-1, which are important mediators of endocytosis [37]. It is noteworthy that Rab5C

miR-133a-3p in lung squamous cell carcinoma

Table 3. KEGG pathway enriched of miR-133a-3p target genes

Term ID	Description	Count	<i>p</i> -value	Genes
hsa04144	Endocytosis	15	0.0048	PARD6B, CLTA, ARFGAP3, PARD3, FGFR3, RAB5C, TGFBR1, PSD3, VPS37D, LDLRAP1, CDC42, ADRB1, VPS4B, MDM2, EHD1
hsa04520	Adherens junction	8	0.0175	FGFR1, CDC42, TCF7, PARD3, TGFBR1, WASF2, CTNND1, IQGAP1
hsa00510	N-Glycan biosynthesis	6	0.0213	RFT1, MAN1A2, FUT8, DPM2, ALG6, DOLPP1
hsa04115	p53 signaling pathway	7	0.0308	CDKN1A, TNFRSF10B, SHISA5, SERPINE1, MDM2, CHEK1, PERP
hsa04150	mTOR signaling pathway	6	0.0342	EIF4B, RPS6KA3, ULK1, IGF2, RPS6KB1, PRKAA2
hsa04810	Regulation of actin cytoskeleton	14	0.0373	FGFR1, FGFR3, PDGFA, WASF2, RDX, IGF2, ARPC5, MYH9, VAV2, IQGAP1, ARPC1A, CDC42, MSN, FGF1
hsa00760	Nicotinate and nicotinamide metabolism	4	0.0498	AOX1, NADK, NT5E, NMNAT1

(belonging to the same family of Rab5A) and LDLRAP1 (belonging to the same family of LDLR) are the target genes of miR-133a-3p in the current study and are enriched in endocytosis. New insight into the mechanism in LUSC maybe found through GO and KEGG pathway enrichment analyses.

However, some limitations exist in the current study. First, the sample size of the validated cohort was not sufficiently large, and all of the samples are FFPE tissues, instead of fresh tissue samples. There may be some effects on miR-133a-3p expression. Second, heterogeneity was found among the included studies in the meta-analysis. In addition to the regional factors, diversity in sample size, different quality and an inconsistent platform are also considered to be sources of heterogeneity. However, no publication bias was detected among the included studies; thus, the reliable degrees of the meta-analysis deserved overall consideration.

In conclusion, the current study showed that miR-133a-3p and its pri-miRNAs were down-regulated in LUSC tissues. Combined with the reports mentioned above, we hypothesize that miR-133a-3p plays a role as a tumor suppressor in LUSC. miR-133a-3p is a potential biomarker that is used to diagnose LUSC and is a promising gene in targeted therapy. Functional annotation of the miR-133a-3p target genes provides a new direction to research the molecular mechanism in LUSC. However, more effort is still needed for further investigations.

Acknowledgements

The study was supported by Fund of the Guangxi Provincial Health Bureau Scientific Research Project (Z2013201, Z2014055), Fund of the National Natural Science Foundation of China (NSFC81360327, NSFC81560469), the Natural Science Foundation of Guangxi, China (2015GXNSFCA139009), the Natural Science Foundation of Guangxi, China (2016-GXNSFAA380255). The authors thank the GEO Dataset and TCGA database for offering the data for this study.

Disclosure of conflict of interest

None.

Address correspondence to: Gang Chen and Dianzhong Luo, Department of Pathology, First Affili-

ated Hospital of Guangxi Medical University, 6 Shuangyong Road, Nanning 530021, Guangxi Zhuang Autonomous Region, China. Fax: 0086-771-5356534; E-mail: chen_gang_triones@163.com (GC); 13878802796@163.com (DZL)

References

- [1] Parkin DM, Laara E and Muir CS. Estimates of the worldwide frequency of sixteen major cancers in 1980. *Int J Cancer* 1988; 41: 184-197.
- [2] Ferlay J, Soerjomataram I, Dikshit R, Eser S, Mathers C, Rebelo M, Parkin DM, Forman D and Bray F. Cancer incidence and mortality worldwide: sources, methods and major patterns in GLOBOCAN 2012. *Int J Cancer* 2015; 136: E359-386.
- [3] Billmeier SE, Ayanian JZ, Zaslavsky AM, Nerenz DR, Jaklitsch MT and Rogers SO. Predictors and outcomes of limited resection for early-stage non-small cell lung cancer. *J Natl Cancer Inst* 2011; 103: 1621-1629.
- [4] Mosti G and Partsch H. Improvement of venous pumping function by double progressive compression stockings: higher pressure over the calf is more important than a graduated pressure profile. *Eur J Vasc Endovasc Surg* 2014; 47: 545-549.
- [5] Tan DS, Camilleri-Broet S, Tan EH, Alifano M, Lim WT, Bobbio A, Zhang S, Ng QS, Ang MK, Iyer NG, Takano A, Lim KH, Regnard JF, Tan P and Broet P. Intertumor heterogeneity of non-small-cell lung carcinomas revealed by multiplexed mutation profiling and integrative genomics. *Int J Cancer* 2014; 135: 1092-1100.
- [6] Lovat F, Valeri N and Croce CM. MicroRNAs in the pathogenesis of cancer. *Semin Oncol* 2011; 38: 724-733.
- [7] Lujambio A and Lowe SW. The microcosmos of cancer. *Nature* 2012; 482: 347-355.
- [8] Fabbri M, Garzon R, Cimmino A, Liu Z, Zanasi N, Callegari E, Liu S, Alder H, Costinean S, Fernandez-Cymering C, Volinia S, Guler G, Morrison CD, Chan KK, Marcucci G, Calin GA, Huebner K and Croce CM. MicroRNA-29 family reverts aberrant methylation in lung cancer by targeting DNA methyltransferases 3A and 3B. *Proc Natl Acad Sci U S A* 2007; 104: 15805-15810.
- [9] Guo W, Wang Q, Zhan Y, Chen X, Yu Q, Zhang J, Wang Y, Xu XJ and Zhu L. Transcriptome sequencing uncovers a three-long noncoding RNA signature in predicting breast cancer survival. *Sci Rep* 2016; 6: 27931.
- [10] Shen ED, Liu B, Yu XS, Xiang ZF and Huang HY. The effects of miR-1207-5p expression in peripheral blood on cisplatin-based chemosensitivity of primary gallbladder carcinoma. *Oncotargets Ther* 2016; 9: 3633-3642.

miR-133a-3p in lung squamous cell carcinoma

- [11] de Melo Maia B, Rodrigues IS, Akagi EM, Soares do Amaral N, Ling H, Monroig P, Soares FA, Calin GA and Rocha RM. MiR-223-5p works as an oncomiR in vulvar carcinoma by TP63 suppression. *Oncotarget* 2016; [Epub ahead of print].
- [12] Flores-Perez A, Marchat LA, Rodriguez-Cuevas S, Bautista VP, Fuentes-Mera L, Romero-Zamora D, Maciel-Dominguez A, de la Cruz OH, Fonseca-Sanchez M, Ruiz-Garcia E, la Vega HA and Lopez-Camarillo C. Suppression of cell migration is promoted by miR-944 through targeting of SIAH1 and PTP4A1 in breast cancer cells. *BMC Cancer* 2016; 16: 379.
- [13] Moriya Y, Nohata N, Kinoshita T, Mutallip M, Okamoto T, Yoshida S, Suzuki M, Yoshino I and Seki N. Tumor suppressive microRNA-133a regulates novel molecular networks in lung squamous cell carcinoma. *J Hum Genet* 2012; 57: 38-45.
- [14] Mirghasemi A, Taheriazam A, Karbasy SH, Torkaman A, Shakeri M, Yahaghi E and Mokarizadeh A. Down-regulation of miR-133a and miR-539 are associated with unfavorable prognosis in patients suffering from osteosarcoma. *Cancer Cell Int* 2015; 15: 86.
- [15] Zhang W, Liu K, Liu S, Ji B, Wang Y and Liu Y. MicroRNA-133a functions as a tumor suppressor by targeting IGF-1R in hepatocellular carcinoma. *Tumour Biol* 2015; 36: 9779-9788.
- [16] Wang Y, Li J, Chen H, Mo Y, Ye H, Luo Y, Guo K, Mai Z, Zhang Y, Chen B, Zhou Y and Yang Z. Down-regulation of miR-133a as a poor prognosticator in non-small cell lung cancer. *Gene* 2016; 591: 333-7.
- [17] Lan D, Zhang X, He R, Tang R, Li P, He Q and Chen G. MiR-133a is downregulated in non-small cell lung cancer: a study of clinical significance. *Eur J Med Res* 2015; 20: 50.
- [18] Mataka H, Enokida H, Chiyomaru T, Mizuno K, Matsushita R, Goto Y, Nishikawa R, Higashimoto I, Samukawa T, Nakagawa M, Inoue H and Seki N. Downregulation of the microRNA-1/133a cluster enhances cancer cell migration and invasion in lung-squamous cell carcinoma via regulation of Coronin1C. *J Hum Genet* 2015; 60: 53-61.
- [19] Sarkar D, Parkin R, Wyman S, Bendoraite A, Sather C, Delrow J, Godwin AK, Drescher C, Huber W, Gentleman R and Tewari M. Quality assessment and data analysis for microRNA expression arrays. *Nucleic Acids Res* 2009; 37: e17.
- [20] Ritchie ME, Phipson B, Wu D, Hu Y, Law CW, Shi W and Smyth GK. limma powers differential expression analyses for RNA-sequencing and microarray studies. *Nucleic Acids Res* 2015; 43: e47.
- [21] Chen G, Umelo IA, Lv S, Teugels E, Fostier K, Kronenberger P, Dewaele A, Sadones J, Geers C and De Greve J. miR-146a inhibits cell growth, cell migration and induces apoptosis in non-small cell lung cancer cells. *PLoS One* 2013; 8: e60317.
- [22] Dang YW, Zeng J, He RQ, Rong MH, Luo DZ and Chen G. Effects of miR-152 on cell growth inhibition, motility suppression and apoptosis induction in hepatocellular carcinoma cells. *Asian Pac J Cancer Prev* 2014; 15: 4969-4976.
- [23] Cancer Genome Atlas Research N. Comprehensive genomic characterization of squamous cell lung cancers. *Nature* 2012; 489: 519-525.
- [24] Mizuno K, Seki N, Mataka H, Matsushita R, Kamikawaji K, Kumamoto T, Takagi K, Goto Y, Nishikawa R, Kato M, Enokida H, Nakagawa M and Inoue H. Tumor-suppressive microRNA-29 family inhibits cancer cell migration and invasion directly targeting LOXL2 in lung squamous cell carcinoma. *Int J Oncol* 2016; 48: 450-460.
- [25] Zhang X, Li P, Rong M, He R, Hou X, Xie Y and Chen G. MicroRNA-141 is a biomarker for progression of squamous cell carcinoma and adenocarcinoma of the lung: clinical analysis of 125 patients. *Tohoku J Exp Med* 2015; 235: 161-169.
- [26] Hou Z, Xu C, Xie H, Xu H, Zhan P, Yu L and Fang X. Long noncoding RNAs expression patterns associated with chemo response to cisplatin based chemotherapy in lung squamous cell carcinoma patients. *PLoS One* 2014; 9: e108133.
- [27] Ma J, Lin Y, Zhan M, Mann DL, Stass SA and Jiang F. Differential miRNA expressions in peripheral blood mononuclear cells for diagnosis of lung cancer. *Lab Invest* 2015; 95: 1197-1206.
- [28] Mavridis K, Gueugnon F, Petit-Courty A, Courty Y, Barascu A, Guyetant S and Scorilas A. The oncomiR miR-197 is a novel prognostic indicator for non-small cell lung cancer patients. *Br J Cancer* 2015; 112: 1527-1535.
- [29] Wang Y, Li J, Chen H, Mo Y, Ye H, Luo Y, Guo K, Mai Z, Zhang Y, Chen B, Zhou Y and Yang Z. Down-regulation of miR-133a as a poor prognosticator in non-small cell lung cancer. *Gene* 2016; 591: 333-7.
- [30] Petriella D, De Summa S, Lacalamita R, Galetta D, Catino A, Logroscino AF, Palumbo O, Carella M, Zito FA, Simone G and Tommasi S. miRNA profiling in serum and tissue samples to assess noninvasive biomarkers for NSCLC clinical outcome. *Tumour Biol* 2016; 37: 5503-5513.
- [31] Wang LK, Hsiao TH, Hong TM, Chen HY, Kao SH, Wang WL, Yu SL, Lin CW and Yang PC. MicroRNA-133a suppresses multiple oncogenic membrane receptors and cell invasion in non-small cell lung carcinoma. *PLoS One* 2014; 9: e96765.

miR-133a-3p in lung squamous cell carcinoma

- [32] Yuan Y, Yao YF, Hu SN, Gao J and Zhang LL. MiR-133a Is Functionally Involved in Doxorubicin-Resistance in Breast Cancer Cells MCF-7 via Its Regulation of the Expression of Uncoupling Protein 2. *PLoS One* 2015; 10: e0129843.
- [33] Zhou Y, Wu D, Tao J, Qu P, Zhou Z and Hou J. MicroRNA-133 inhibits cell proliferation, migration and invasion by targeting epidermal growth factor receptor and its downstream effector proteins in bladder cancer. *Scand J Urol* 2013; 47: 423-432.
- [34] Yang Y, Gao W, Ding X, Xu W, Liu D, Su B and Sun Y. Variations within 3'-UTR of MDM4 gene contribute to clinical outcomes of advanced non-small cell lung cancer patients following platinum-based chemotherapy. *Oncotarget* 2016; [Epub ahead of print].
- [35] Jinesh GG and Kamat AM. Endocytosis and serpentine filopodia drive blebbistatin-mediated resurrection of apoptotic cancer stem cells. *Cell Death Discov* 2016; 2.
- [36] Vilema-Enriquez G, Arroyo A, Grijalva M, Amador-Zafra RI and Camacho J. Molecular and Cellular Effects of Hydrogen Peroxide on Human Lung Cancer Cells: Potential Therapeutic Implications. *Oxid Med Cell Longev* 2016; 2016: 1908164.
- [37] Aranda JF, Canfran-Duque A, Goedeke L, Suarez Y and Fernandez-Hernando C. The miR-199-dynamin regulatory axis controls receptor-mediated endocytosis. *J Cell Sci* 2015; 128: 3197-3209.